

# Improved Hodgkin & Huxley-type model for action potentials in squid

P. J. Stiles (1) and C. G. Gray (2)

((1) Department of Molecular Sciences, Macquarie University, Australia,  
(2) Department of Physics, University of Guelph, Canada)

## Abstract

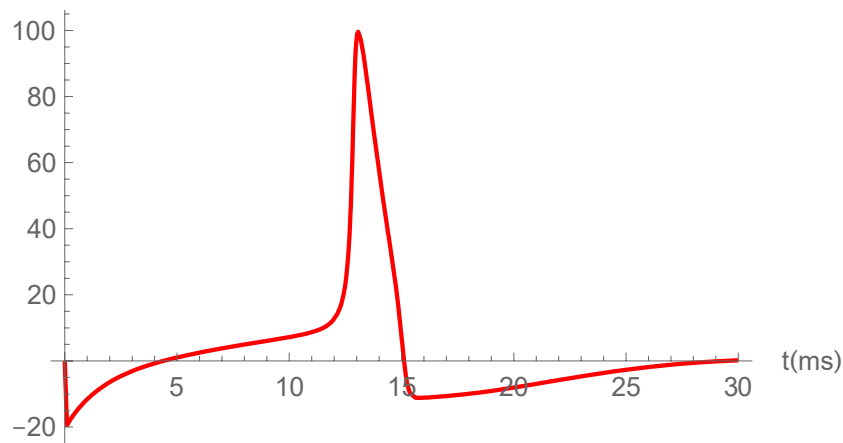
By extending the crude Goldman-Hodgkin-Katz electrodiffusion model for resting-state membrane potentials in perfused axons of squid we reformulate the Hodgkin-Huxley (HH) phenomenological quantitative model to create a model which is simpler, more quantitative, and based more fundamentally on electrodiffusion principles. Our dynamical system, like that of HH, behaves as a 4-dimensional resonator exhibiting subthreshold oscillations. Speeds of propagating action potentials at 20°C are in very good agreement with the HH experimental value at 18.5°C. Unlike its HH counterpart it does not predict spike trains during prolonged constant-current stimulation, in agreement with recent experiments. Our resonator model predicts rebound spiking following prolonged hyperpolarizing stimulation, observed at 18.5°C by HH but not predicted at this temperature by their quantitative model. Spiking promoted by brief (0.1 ms) hyperpolarization is also predicted at room temperature by our electrodiffusion model but only at much lower temperatures (*ca.* 6°C) by the HH model. Such spiking in giant axons induced directly by brief hyperpolarizing stimulation at room temperature does not appear to have been investigated experimentally for either stationary membrane action potentials or their propagating counterparts.

## 1. Introduction

In a superb pioneering contribution to computational biology Hodgkin and Huxley (HH) proposed a quantitative model [1] for the initiation and propagation of action potentials in the giant axon of squid. Transient electric-current and steady-state responses of giant axons, initially in their resting states, to a range of clamped membrane potentials were recorded [2] and fitted [1] to a highly empirical dynamical system of first-order nonlinear differential equations in the time dependent membrane depolarization  $V(t)$ , sodium-channel gating functions  $m(t)$  and  $h(t)$ , and a potassium-channel gating function  $n(t)$ . Each gating function refers to the fraction of open ion gates in a macroscopic sample of the axonal membrane. Relatively recent experiments on squid giant axons by Clay [3] indicate that trains of action potentials, predicted by the HH quantitative model during prolonged constant electric current stimulation are not observed, at least in perfused axons. Our present theoretical model supports his claim. Nevertheless, earlier observations by I. Tasaki [4] and Chapman [5] suggest that spike trains can be observed during prolonged stimulation of freshly dissected nerve fibers. The HH quantitative model successfully predicts membrane action potentials in ‘anode-break excitation’ or ‘rebound spiking’ experiments at 6.3°C in which a *prolonged* transverse hyperpolarizing electric current stimulus is abruptly terminated. It fails, however,

to account for the same phenomenon at 18.5 °C where resonator behavior [6,7] might be expected to be enhanced by lower translational ionic friction. It is not widely appreciated that the HH quantitative model for rebound spiking predicts a normal membrane action potential at 6.3 °C in response to a *very brief* ( 0.1 ms) hyperpolarizing current stimulus (see Fig. 1A) applied to the axonal membrane, a phenomenon fundamental to the notion of facilitatory roles for inhibitory synaptic inputs [8] in neural networks. This phenomenon, too, is not predicted at higher temperatures such as 20 °C by the HH model but, as shown in Fig.1B below, is certainly predicted at this temperature by the resonator version of our simpler electrodiffusion model. Both models exhibit underdamped subthreshold oscillations,

**A** action potential  $V(t)$  (mV)



**B** action potential  $V(t)$  (mV)

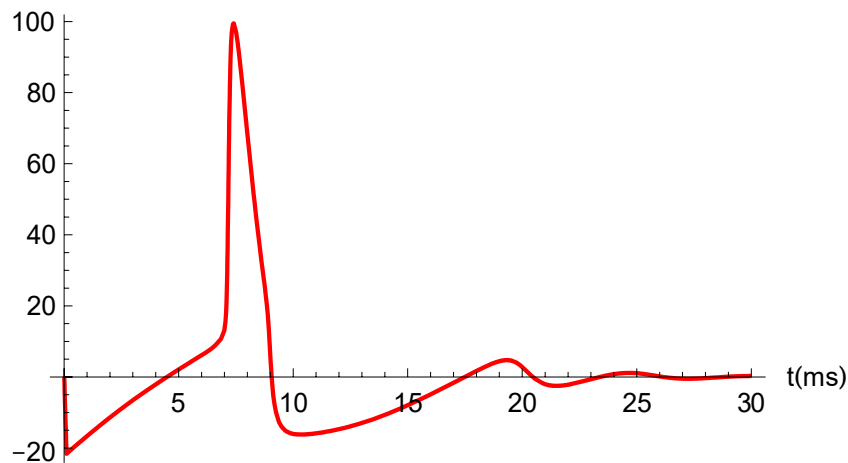


Fig.1. The membrane action potential (A) predicted by the well-known HH quantitative model when a squid axon, initially in its resting state, fires in response to a constant 0.1 ms inhibitory hyperpolarizing current pulse of strength  $200 \mu\text{A cm}^{-2}$  at 6.3 °C . The corresponding membrane action potential (B) predicted at 20 °C by our new electrodiffusion model in response to a 0.1 ms hyperpolarizing current stimulus of strength  $220 \mu\text{A cm}^{-2}$  .

characteristic of resonators [6,7], as well as resonate-and-fire action potential generation [7,9] in response to a very brief superthreshold depolarizing or hyperpolarizing electric perturbation to the resting state.

We model axonal spiking in squid more physically than the phenomenological curve-fitting approach to ion conductance adopted by HH by replacing their *ad hoc*  $m^3h$  and  $n^4$  gating dependencies for sodium- and potassium-ion current densities, respectively, through a more natural extension to the electrodiffusion model [10] of Goldman, Hodgkin and Katz (GHK) [11,12]. We present a particularly natural alternative model for action potentials in the spirit of GHK who used a constant electric-field approximation [11,13] to simplify the Nernst-Planck equations for electrodiffusive transmembrane ion currents in the resting state of a nerve fiber. In this model for action potentials in a perfused [14] squid axon we imagine that the ubiquitous Na-K-ATPase pumps have been rendered inoperative, so coupling of our passive electrodiffusive fluxes to the active pump fluxes [15-18] is artificially suppressed (e.g., by blockers, poisons, or ATP removal). The model can be extended to re-introduce this bioenergetic coupling which prevents a live squid axon from slowly running down towards a state of thermodynamic equilibrium in which action potentials (spikes) can no longer be generated. Although HH disregarded the GHK model in their celebrated quantitative model for action potentials in squid [1], a subsequent GHK-like model of Frankenhaeuser and Huxley [19] still retained arbitrary HH-like  $m^2h$  and  $n^2$  gating dependencies for sodium- and potassium-ion current densities which our present model, outlined below, seeks to avoid. In our electrodiffusion model for channel current-densities some important nonlinearities are naturally expressed in terms of ion permeabilities which are exponential functions of potentials of mean force (PMFs)  $w$  for ions in their specific channels. The PMFs  $w_{\text{Na}}(t)$  and  $w_{\text{K}}(t)$  for sodium and potassium ions depend linearly on the gating functions  $m(t)$ ,  $h(t)$  and  $n(t)$  in our generalized GHK description, and, due to the channels being voltage-gated, the gating functions in turn depend on the membrane depolarization  $V(t)$  which is time-dependent when the membrane is not at steady-state.

As far as we are aware, apart from a precursor [20] to this paper, ours is the first four-variable model to improve, as well as simplify, the HH treatment for squid. There have been numerous two-variable models proposed [7], which simplify visualization of the complicated nonlinear dynamics in a four dimensional phase space, and with the aid of approximations, reduce the dynamics to a two-dimensional phase plane.

Consider the electric current density  $i$  of an ion species of charge  $q$  in an idealized dedicated ion channel with axis  $x$  spanning the axonal membrane of thickness  $L$ . If  $e$  represents the proton charge then  $q = +e$  for sodium and potassium ions and  $q = -e$  for chloride ions. Our idealized ion channels for each ionic species are cylindrical pores with symmetry axes orthogonal to the membrane surfaces. Such channels are assumed to account for a surface fraction  $f$  of the membrane area. We assume model channels perfectly selective for ions of a given species; this is a reasonable first approximation since [21], under normal conditions, Na channels are selective for  $\text{Na}^+$  ions over  $\text{K}^+$  ions by 12:1, K channels are very selective for  $\text{K}^+$  ions over  $\text{Na}^+$  ions by orders of magnitude and these channels are all very selective with respect to charge sign (perm-selective). The Nernst-Planck-Kramers equation [10] for electrodiffusion of ions with an average intra-channel number-density  $c(x,t)$  at an axial position  $x$  and time  $t$  tells us that the membrane current-density  $i(x,t)$  for a particular ion passing through its specific channel is

$$i(x,t) = -q f D \left( \partial c(x,t) / \partial x + \beta c(x,t) \partial w_{\text{tot}}(x,t) / \partial x \right) \quad , \quad (1)$$

where  $D$ , assumed constant, is the ion diffusion coefficient in its specific channel,  $w_{\text{tot}}(x, t)$  is the total PMF of the ion of interest in its specific channel, and the coefficient  $\beta = 1/k_{\text{B}}T$  is defined in terms of the Boltzmann constant  $k_{\text{B}}$  and the absolute temperature  $T$ . The terms proportional to  $\partial c / \partial x$  and  $\partial w_{\text{tot}} / \partial x$  in (1) are called the “diffusion” and “drift” terms respectively. We regard the PMF  $w_{\text{tot}}(x, t)$  of a channel ion as the sum of an electrostatic contribution  $q\phi(x, t)$  from the electrostatic potential  $\phi(x, t)$  in the essentially one-dimensional ion channel and a second contribution  $w(x, t)$  from all other forces between the permeant ion and its channel, including the electric polarization energy. Following Goldman [11,12] we replace the local axial electric field  $E(x, t) = -\partial\phi(x, t) / \partial x$  in a channel by a constant value, its spatially averaged value between the internal cytoplasmic membrane interface  $x = 0$  and the external interface at  $x = L$ , and write  $E(x, t) = V_{\text{m}}(t) / L \equiv E(t)$ . The electric potential difference  $\phi(0, t) - \phi(L, t)$  defines the physiological membrane potential  $V_{\text{m}}(t)$ . For the resting state of the axonal membrane of squid the membrane potential  $V_{\text{m}} = V_{\text{rest}}$  is negative and takes an experimental value [22] close to  $-70$  mV at  $20^\circ\text{C}$  for the normal resting state, i.e., with sodium-potassium pumps operating. As we discuss below, the resting potential in the perfused state with these pumps off [15,18] is closer to  $-68$  mV at  $20^\circ\text{C}$ . The depolarization  $V(t)$  at time  $t$  is defined by  $V(t) = V_{\text{m}}(t) - V_{\text{rest}}$ . A neural membrane is said to be depolarized if  $V(t) > 0$  and to be hyperpolarized when  $V(t) < 0$ . Using the Goldman constant-field approximation [11] we find that the quasi-steady-state solution to (1), regarded as an ordinary first-order differential equation with fixed boundary conditions  $c(0, t) = c^{\text{int}}$  at  $x = 0$  and  $c(L, t) = c^{\text{ext}}$  at  $x = L$ , takes the form [10]

$$i(t) = \frac{q f D (c^{\text{int}} - c^{\text{ext}} \exp(-\beta q V_{\text{m}}(t)))}{\int_0^L \exp(\beta (w(x, t) - q(x/L) V_{\text{m}}(t))) dx}, \quad (2)$$

where, with our choice of coordinate system, outward current is positive.

We adopt the simplest possible model for the PMF and assume  $w(x, t)$  inside a channel is spatially constant so that  $w(x, t) = w(t)$ . This PMF  $w$  is assumed to vanish outside the channel. For chloride channels we assume no gating and therefore take  $w_{\text{Cl}}$  to be independent of time. For potassium and sodium channels the spatially constant value of each PMF depends on whether the channel is open, closed, or transitioning between these states. Temporal gating of potassium channels and sodium channels leads to PMFs  $w_{\text{K}}(t)$  and  $w_{\text{Na}}(t)$  respectively. In the channels of the monovalent cations sodium and potassium,  $q = e$ , so that (2) reduces to

$$i(t) = \frac{\beta e^2 V_{\text{m}}(t) P(t) (c^{\text{int}} - c^{\text{ext}} \exp(-\beta e V_{\text{m}}(t)))}{1 - \exp(-\beta e V_{\text{m}}(t))}, \quad (3)$$

a simple extension of the traditional resting-state version of the GHK equation for ionic current densities in which both the resting membrane potential  $V_{\text{m}} = V_{\text{rest}}$  and the ion

permeabilities  $P$  have been replaced by their dynamic generalizations  $V_m(t)$  and  $P(t)$  which vary on a millisecond timescale. The latter take the form

$$P_{\text{Na}}(t) = (f_{\text{Na}} D_{\text{Na}} / L) \exp(-\beta w_{\text{Na}}(t)) , \quad (4a)$$

$$P_{\text{K}}(t) = (f_{\text{K}} D_{\text{K}} / L) \exp(-\beta w_{\text{K}}(t)) . \quad (4b)$$

In the absence of chloride-channel gating the chloride ion permeability takes the constant value

$$P_{\text{Cl}} = (f_{\text{Cl}} D_{\text{Cl}} / L) \exp(-\beta w_{\text{Cl}}) . \quad (4c)$$

In (4a) and (4b) the cation PMFs  $w_{\text{Na}}$  and  $w_{\text{K}}$ , depend, on the action potential  $V(t)$  through the time-dependent gating functions  $m(t)$ ,  $h(t)$  and  $n(t)$ . It follows that the cation permeabilities  $P_{\text{Na}}$  and  $P_{\text{K}}$  are also functions of time. For potassium ion channels we write the PMF as

$$w_{\text{K}}(t) = n(t) w_{\text{K}}^{\text{O}} + (1 - n(t)) w_{\text{K}}^{\text{C}} , \quad (5)$$

where  $n(t)$  is the fraction of open potassium gates at time  $t$ ,  $w_{\text{K}}^{\text{O}}$  is the PMF of a K channel with a fully open ( $n = 1$ ) gate, and  $w_{\text{K}}^{\text{C}}$  is the K channel PMF with a completely closed ( $n = 0$ ) gate. As we discuss below, the gating functions such as  $n$  depend on the membrane potential  $V_m$ . Thus  $n = n(V_m)$  and in the time-dependent case  $n(t)$  can also be denoted as  $n(V_m(t))$  or  $n(V(t))$ . These PMFs are measured relative to that of a potassium ion in the external bulk electrolyte. Similarly, for sodium-ion channels we define

$$w_{\text{Na}}(t) = m(t) w_{\text{Na}}^{\text{O}} + (1 - m(t)) w_{\text{Na}}^{\text{C}} + h(t) w_{\text{Na}}^{\dagger\text{O}} + (1 - h(t)) w_{\text{Na}}^{\dagger\text{C}} , \quad (6)$$

where  $m(t)$  refers to the fraction of open activation gates and  $h(t)$  to the fraction of open inactivation gates. The four Na channel PMFs  $w_{\text{Na}}^{\text{C}}$ ,  $w_{\text{Na}}^{\text{O}}$ ,  $w_{\text{Na}}^{\dagger\text{C}}$  and  $w_{\text{Na}}^{\dagger\text{O}}$  refer, respectively, to the completely closed ( $m = 0$ ) and completely open ( $m = 1$ ) states of the sodium activation gate, and to the completely closed ( $h = 0$ ) and completely open ( $h = 1$ ) states of the sodium inactivation gate. The formalism of HH [1] suggests that the sodium- and potassium-channel resting state gating functions with the Na-K-ATPase pumps on are  $m(V = 0) \approx 0.053$ ,  $h(V = 0) \approx 0.60$  and  $n(V = 0) \approx 0.32$  at  $20^\circ\text{C}$  but we shall see that a somewhat different picture emerges from our own electrodiffusion formalism when the excitable membrane is initially in its perfused resting state [14]. In the following section we discuss our version of gating kinetics inspired by, but simpler than the first-order scheme originally proposed by HH. An action potential of amplitude  $V_m(t)$  is generated when gating kinetics causes the potentials of mean force  $w_{\text{Na}}(t)$  and  $w_{\text{K}}(t)$  for the cation channels to be appropriately synchronized.

## 2. Resting Potentials and Action Potentials

Magnetic fields due to intra-membrane currents are normally negligible because the speeds of ions traversing the axonal membrane are so small. Thus, in the dissipative resting state of the membrane the sum of the electrodiffusive steady-state chloride, sodium and potassium ion current densities is zero, as demanded by the magnetic-field free version of the Maxwell equation,  $\partial D_x / \partial t = -i_{\text{tot}} = -(i_{\text{Cl}} + i_{\text{Na}} + i_{\text{K}}) = 0$  for the temporal derivative of the x-component, perpendicular to the membrane surface, of the electric displacement field  $\mathbf{D}$ . From the resting-state version of (3) we then find that the GHK resting potential [11,12] is given by the well-known expression

$$V_{\text{rest}} = \frac{k_{\text{B}}T}{e} \ln \left[ \frac{P_{\text{Na}}c_{\text{Na}}^{\text{ext}} + P_{\text{K}}c_{\text{K}}^{\text{ext}} + P_{\text{Cl}}c_{\text{Cl}}^{\text{int}}}{P_{\text{Na}}c_{\text{Na}}^{\text{int}} + P_{\text{K}}c_{\text{K}}^{\text{int}} + P_{\text{Cl}}c_{\text{Cl}}^{\text{ext}}} \right] . \quad (7)$$

For our model the constant resting-state permeabilities in (7) at time  $t = 0$  are given by

$$P_{\text{Na}} = (f_{\text{Na}} D_{\text{Na}} / L) \exp(-\beta w_{\text{Na}}(0)) , \quad (8a)$$

$$P_{\text{K}} = (f_{\text{K}} D_{\text{K}} / L) \exp(-\beta w_{\text{K}}(0)) , \quad (8b)$$

and

$$P_{\text{Cl}} = (f_{\text{Cl}} D_{\text{Cl}} / L) \exp(-\beta w_{\text{Cl}}) . \quad (8c)$$

When transmembrane ion currents are time-dependent the membrane potential  $V_{\text{m}}(t) = V_{\text{rest}} + V(t)$  also becomes a function of time. A characteristic temporal response  $V(t)$  of the local membrane potential, known as the membrane action potential [1] or space-clamped action potential, is observed in a small region of an excitable membrane whenever such a region is depolarized by an external electric stimulus with a magnitude exceeding some value (not always precisely the same). For action potentials associated primarily with gating of sodium channels we might expect the action potential depolarization threshold to occur in the region of  $V$  where the sodium activation gating variable  $m(V)$  begins to rise most steeply from near zero towards unity ( $V \sim 6$  mV for our squid axon as seen in Fig. 2 below). Our analysis, indeed, reveals a very narrow threshold beginning at 6.560 mV for our resonator model of the squid axon. We refer to [7] for a detailed discussion of the distinctions between “resonator” and “integrator” neurons; [6] gives a brief discussion of one important distinction. The question of whether such a threshold for the initiation of an isolated action potential is mathematically sharp has long been debated [1,7,23,24]. Theoretical models for resonators [7], such as that of HH suggest that at least for squid, an action potential can be initiated for depolarizations in an extremely narrow distribution of threshold values, sometimes called a fuzzy threshold. For integrators with a second fixed point, unstable and near the resting potential [7], one might expect an even sharper threshold. The stimulus for action potential generation frequently takes the form of an initially applied depolarizing voltage shock,  $V(0) = V_{\text{stim}}$ , or of a transverse depolarizing electric current-density,  $i_{\text{stim}}(t)$  injected briefly into the membrane. Like the electrodiffusive resting

potential, the space-clamped membrane action potential can also be predicted from the Maxwell equation (in SI)

$$\partial D_x / \partial t = (\varepsilon_m \varepsilon_0 / L) \partial V_m / \partial t = -i_{\text{tot}}(t) \quad , \quad (9a)$$

or equivalently

$$C_m \dot{V} = -(i_{\text{stim}}(t) + i_{\text{Cl}}(t) + i_{\text{Na}}(t) + i_{\text{K}}(t)) \quad , \quad (9b)$$

where  $C_m = \varepsilon_m \varepsilon_0 / L$  represents the membrane capacitance per unit area,  $\varepsilon_m$  is the membrane relative permittivity (dielectric constant),  $\varepsilon_0$  is the permittivity of free space, and  $\dot{V} = dV / dt$ . The symbol  $i_{\text{tot}}(t)$  in (9a) refers to the sum of any stimulating current-density,  $i_{\text{stim}}(t)$ , and the current densities of all other permeant ions. Using (3) - (6) we can express all time-dependent ionic current densities in (9b) in terms of the resting potential, the time-dependent membrane depolarization  $V(t)$ , the sodium-channel gating functions  $m(t)$  and  $h(t)$ , and the potassium-channel gating function  $n(t)$ .

HH [1] assumed that the sodium-channel gating was determined exclusively by the membrane potential through the first-order relaxation equations

$$\dot{m} = (m_{\text{ss}}(V) - m(t)) / \tau_m(V) \quad , \quad (10a)$$

and

$$\dot{h} = (h_{\text{ss}}(V) - h(t)) / \tau_h(V) \quad , \quad (10b)$$

where  $m_{\text{ss}}(V)$  and  $\tau_m(V)$ , together with  $h_{\text{ss}}(V)$  and  $\tau_h(V)$ , refer to values of steady-state gating functions and relaxation times, respectively, for the activation and inactivation gates when the membrane depolarization is  $V$ . Subsequent investigations [25-27] indicated that sodium inactivation gating in squid is directly related to the activation gating but only indirectly to the membrane potential. Although the extent of direct voltage involvement in sodium channel inactivation gating for squid remains somewhat controversial [26], we have suggested [10] that it may be useful to replace  $h_{\text{ss}}(V)$  in (10b) by  $h_{\text{ss}}(m)$  where  $m$  is a function of  $V$ . If we further assume that all gating relaxation times can be regarded as constant [10], equations (10a) and (10b) can be replaced by their simpler versions

$$\dot{m} = (m_{\text{ss}}(V) - m(t)) / \tau_m \quad , \quad (11a)$$

and

$$\dot{h} = (h_{\text{ss}}(m) - h(t)) / \tau_h \quad , \quad (11b)$$

respectively. We also replace the HH relaxation equation  $\dot{n} = (n_{\text{ss}}(V) - n(t)) / \tau_n(V)$  for potassium-channel gating by its simpler counterpart

$$\dot{n} = (n_{ss}(V) - n(t)) / \tau_n \quad , \quad (11c)$$

where  $\tau_n$  is assumed constant.

When the stimulus for the generation of an action potential takes the form of a voltage shock the stimulating current-density  $i_{stim}(t)$  can be set to zero. Equation (9b) for the temporal derivative of the membrane depolarization with ion currents defined by (3) – (6), together with the differential equations (11) for ion gating, constitute an autonomous dynamical system of four first-order nonlinear differential equations for the four dynamical variables  $V(t)$ ,  $m(t)$ ,  $h(t)$  and  $n(t)$ . This dynamical system is then completely defined by assigning algebraic forms for the steady-state gating functions  $m_{ss}(V)$ ,  $h_{ss}(m)$  and  $n_{ss}(V)$ , and specifying the seven PMFs  $w_{Na}^O$ ,  $w_{Na}^C$ ,  $w_{Na}^{\dagger O}$ ,  $w_{Na}^{\dagger C}$ ,  $w_K^O$ ,  $w_K^C$  and  $w_{Cl}$ , together with initial conditions on the four dynamical variables. For voltage-shock stimulation of an axon in its resting state these initial conditions take the form  $V(0) = V_{stim}$ ,  $m(0) = m_{rest}$ ,  $h(0) = h_{rest}$  and  $n(0) = n_{rest}$ . Our gating functions are assumed to be of sigmoidal form. Thus, our steady-state sodium gating functions at 20°C are taken to be

$$m_{ss}(V) = (1 + \tanh(0.16(V - 12))) / 2 \quad , \quad (12a)$$

$$h_{ss}(m) = (1 - \tanh(10(m - 0.25))) / 2 \quad , \quad (12b)$$

and the steady-state potassium channel gating function is

$$n_{ss}(V) = (1 + \tanh(0.15V)) / 2 \quad , \quad (12c)$$

with  $V$  measured in mV. These curves, sketched in Fig. 2, ensure that in the perfused resting state of the squid membrane at  $t = 0$ ,  $m(0) \approx 0.021$  so that the sodium  $m$  gates are only slightly open while  $h(0) \approx 0.99$ , ensuring that the sodium  $h$  gates are almost completely open. Our curve (12c) implies that for potassium gating  $n(0) = 0.5$  so, in the resting state of a perfused axon with  $V = 0$ , our potassium channel gate is halfway open, rather than about 32% open as in the HH model described above.

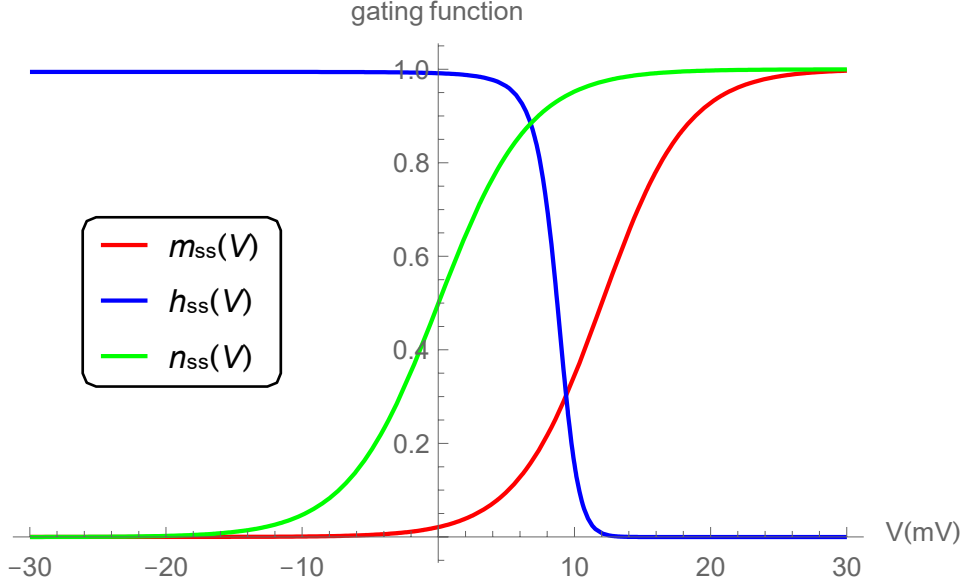


Fig. 2. Our steady-state sodium ion activation gating function  $m_{ss}(V)$  (red), inactivation gating function  $h_{ss}(V)$  (blue) and potassium ion gating function  $n_{ss}(V)$  (green), plotted against membrane depolarization  $V$ .

Other parameters were selected to ensure that the stationary membrane action potentials  $V(t)$  (see Fig. 4) have temporal profiles similar to those recorded by HH. The seven PMFs, three cation gating relaxation times  $\tau$  and channel membrane area fractions  $f$  were also selected by using these criteria and the additional requirement that voltage-clamp electric current transients and steady states should, at least qualitatively, resemble those [1] measured by HH. In Table 1 we list the values of PMFs,  $\tau$  and  $f$  selected for our resonator model at 20°C. Estimates for ion PMFs fall within a range expected from atomistic molecular dynamics simulations [28,29], and our constant gating relaxation times resemble voltage-averaged depolarization-dependent HH values [1]. Our membrane surface fractions occupied by sodium and potassium channels also lie within a broad range supported by experimental studies and rough approximations to cross-sectional areas for these channels [30-32]. Table 1 also contains values of aqueous ion diffusion coefficients  $D$  and bulk concentrations  $c$  of sodium, potassium and chloride ions on each side of a membrane of thickness  $L = 6$  nm and capacitance per unit area  $C_m = 1.0 \mu\text{F cm}^{-2}$  [1,22]

**Table 1. Parameters for permeant ions and channels in our resonator model for the axonal membrane at a notional temperature of 293 K**

Values of  $D$ ,  $c^{\text{int}}$  and  $c^{\text{ext}}$  at 20°C were taken from the literature [10,33] and values of  $f$ ,  $\beta w$  and  $\tau$  were chosen by us according to the criteria outlined following eqs (12). The external medium is regarded as sea water [33].

channel or ion	Na <sup>+</sup>	K <sup>+</sup>	Cl <sup>-</sup>
membrane area fraction ( $10^{-5}$ )	$f_{\text{Na}}$ 10	$f_{\text{K}}$ 3.5	$f_{\text{Cl}}$ 0.5
diffusion coefficient ( $10^{-9} \text{ m}^2\text{s}^{-1}$ )	$D_{\text{Na}}$ 1.19	$D_{\text{K}}$ 1.78	$D_{\text{Cl}}$ 1.84
dimensionless PMF ( $\beta w$ )	$\beta w_{\text{Na}}^{\text{O}}$ 3.0	$\beta w_{\text{K}}^{\text{O}}$ 3.0	$\beta w_{\text{Cl}}$ 6.9
	$\beta w_{\text{Na}}^{\text{C}}$ 12.8	$\beta w_{\text{K}}^{\text{C}}$ 10.9	
	$\beta w_{\text{Na}}^{\text{+O}}, \beta w_{\text{Na}}^{\text{+C}}$		
	-1.8, 8		
ion concentration (mM)	$c_{\text{Na}}^{\text{int}}$ 50	$c_{\text{K}}^{\text{int}}$ 400	$c_{\text{Cl}}^{\text{int}}$ 40
	$c_{\text{Na}}^{\text{ext}}$ 460	$c_{\text{K}}^{\text{ext}}$ 10	$c_{\text{Cl}}^{\text{ext}}$ 540
	$\tau_{\text{m}}, \tau_{\text{h}}$ 0.12, 2.5	$\tau_{\text{n}}$ 2	

Note that both the HH model and our present theoretical model neglect small contributions to electric currents in ion channels due to opening and closing of the gates themselves. Such gating currents [1] are associated with motions of permanent electric multipoles of the channel gates. It is well known [34] that the displacement current  $\partial \mathbf{D} / \partial t$  used to obtain (9b) also contains small contributions due to spatial translations of gating charges and spatial rotations of higher multipole moments of gating structures within the channel proteins.

When we relax the space-clamp conditions that lead to a stationary membrane action potential, propagation of the action potential occurs along a particular direction of the cylindrical  $z$  axis of the axon, which we define as the positive direction. Our previous transmembrane coordinate  $x$  then becomes the radial coordinate  $\rho$ . We discuss below initial and boundary conditions on the potential  $V$  and current  $i$  that determine the propagation direction. From the Maxwell equation, written in the form  $\partial(\nabla \cdot \mathbf{D}) / \partial t + \nabla \cdot \mathbf{i}_{\text{tot}} = 0$ , which implies conservation of charge, it can be established [1,35] that the HH cable equation for a propagating action potential takes the form

$$C_{\text{m}} \frac{\partial V(z,t)}{\partial t} = \frac{a}{2R} \frac{\partial^2 V(z,t)}{\partial z^2} - i_{\rho}(z,t) \quad , \quad (13)$$

a diffusion equation for the membrane depolarization  $V(z,t)$ , together with the radial ionic current density  $i_\rho(z,t)$  due to ions passing through their respective channels acting as a forcing term. As discussed below, the current density  $i_\rho$  depends on  $V$  nonlinearly, as before, so that (13) is a nonlinear propagation equation for the action potential. In (13)  $a$  is the radius of the cylindrical axon and its uniform internal resistivity  $R$  is defined by the longitudinal component of the total current density  $i_z(z,t) = E_z(z,t)/R$ , where  $E_z$  is the longitudinal component of the electric field. In deriving (13) it is assumed [1] that the resistance of the medium external to the axon is negligible compared to the resistance of the axoplasm. This assumption is valid if the external medium has large transverse dimension compared to radius  $a$ .

We take the initial condition on (13) to be the axially uniform resting depolarization  $V(z,0) = 0$ . The initial gating functions for the axon are also taken to be given by their resting-state values  $m(z,0) = m_{ss}(V(z,0))$ ,  $h(z,0) = h_{ss}(m(z,0))$ , and  $n(z,0) = n_{ss}(V(z,0))$  where steady-state values of the gating functions are defined by (12). For longitudinal current injection through the left hand boundary  $z = 0$  of a finite uniformly cylindrical axon of length  $\ell$  the simplest boundary condition consistent with Ohm's law for the axial electric field is

$$\partial V(z,t) / \partial z |_{z=0} = -R i_{z,\text{stim}}(0,t) \quad , \quad (14a)$$

where  $i_{z,\text{stim}}(0,t)$  is a transient stimulating pulse of current density directed from left to right. If no net longitudinal electric current passes through the right-hand side boundary of the axoplasm where  $z = \ell$  the corresponding local boundary condition at  $z = \ell$ , takes the form

$$\partial V(z,t) / \partial z |_{z=\ell} = 0 \quad . \quad (14b)$$

## 2.1 Steady-State Current-Voltage Relation

Using data in Table 1 we solve (7) and (8) for the resting potential and ion permeabilities in the resting state of the perfused axon at  $20^\circ\text{C}$ . The pumps-off resting potential at  $20^\circ\text{C}$  is  $V_{\text{rest}} = -67.7$  mV. This GHK resting potential is somewhat larger than the experimental resting potential of about  $-70$  mV for a freshly dissected squid axon [22], corresponding to the pumps-on scenario. As found here, the resting potential for electrodiffusion with no pumps operating is widely believed to be more positive than in the membrane resting state with the electrogenic Na-K-ATPase pumps turned on [15,18]. For ion permeabilities in the resting state we find  $P_{\text{Na}} = 3.69 \times 10^{-8} \text{ cm s}^{-1}$ ,  $P_{\text{K}} = 9.95 \times 10^{-7} \text{ cm s}^{-1}$  and  $P_{\text{Cl}} = 1.55 \times 10^{-7} \text{ cm s}^{-1}$ . Our ratio  $P_{\text{Na}} : P_{\text{K}} \approx 0.037$  is lower than an experimental estimate [14] of 0.08 and our chloride ion permeability is also lower than an experimental value [36] of  $3.0 \times 10^{-7} \text{ cm s}^{-1}$ . In this context it should also be noted that the analytical GHK model is not only a simplified version of (1) and (2), but is also a mean-field model that should not be expected to accurately describe how particular monatomic cations or anions pass through their channels in single file [37-41]. The GHK resting state of the axon corresponds to a

stable fixed point of our dynamical system and our calculated pumps-off steady state  $I - V$  curve (Fig. 3) shows that this is the only fixed point. A standard stability analysis indicates that this fixed point, like that of the HH dynamical system, is stable. The HHK experimental pumps-on steady state  $I - V$  curve of the squid axon [2] also exhibits just one fixed point. We expect a small quantitative, but not qualitative difference between  $I - V$  curves for the pumps-on and pumps-off cases.

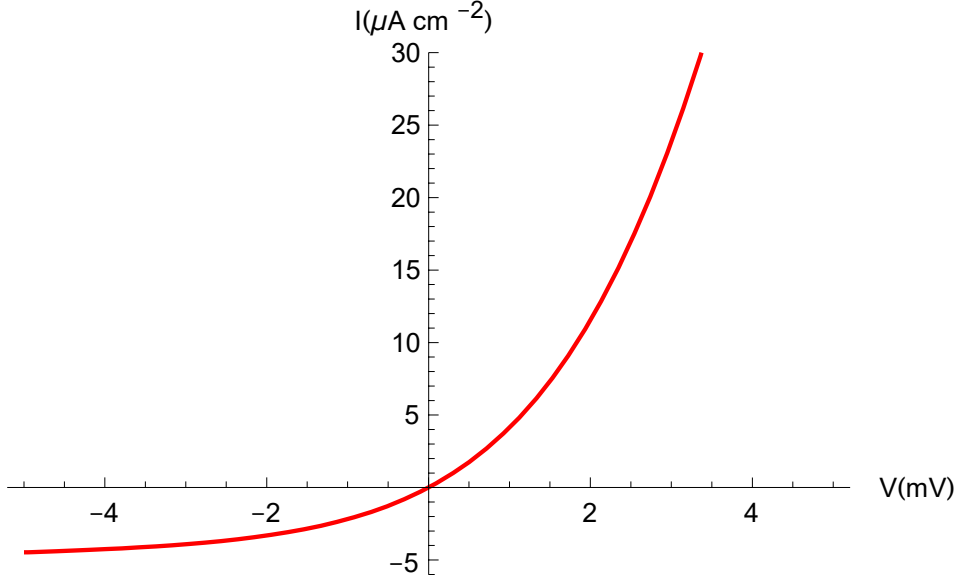


Fig. 3. Plot of the steady-state ion current  $I = i_{\text{Na}}(\infty) + i_{\text{K}}(\infty) + i_{\text{Cl}}(\infty) = -C_m \dot{V}(\infty)$  through the membrane versus membrane depolarization  $V$  showing that the origin representing the resting state of the axon is a fixed point. When the current and voltage axes are extended, no further fixed points become apparent.

Here, the steady-state membrane current  $I$  is related to  $\dot{V}$  in the steady state by (see eqs (9))  $I = i_{\text{tot}}(\infty) = i_{\text{Na}}(\infty) + i_{\text{K}}(\infty) + i_{\text{Cl}}(\infty) = -C_m \dot{V}(\infty)$ . Thus,  $I = 0$  corresponds to one of the four complete steady state conditions,  $\dot{V} = 0$ , which also include  $\dot{m} = 0$ ,  $\dot{h} = 0$  and  $\dot{n} = 0$ . It was from these three latter conditions that Fig. 3 was generated. Fig. 3 shows a plot of our membrane current versus membrane depolarization that is very similar to the experimental [2] pumps-on  $I - V$  curve.

## 2.2 Stationary Membrane Action Potentials

If our model membrane at  $20^\circ\text{C}$  is stimulated by a super threshold depolarizing voltage shock of 14 mV a membrane action potential with a peak height of 119.8 mV ensuing 0.406 ms after the shock is applied, is predicted by (9b) with  $i_{\text{stim}}(t) = 0$  for all  $t$ . A barely superthreshold shock of 6.560 mV produces an action potential with a peak depolarization of only 83.1 mV and a considerably longer latency of 1.75 ms. It is well-known that a brief pulse of depolarizing electric current through the axonal membrane provides a more experimentally convenient alternative method for inducing a membrane action potential. In Fig. 4 we display the membrane action potential induced by a significantly superthreshold depolarizing current density pulse applied for 0.1 ms.

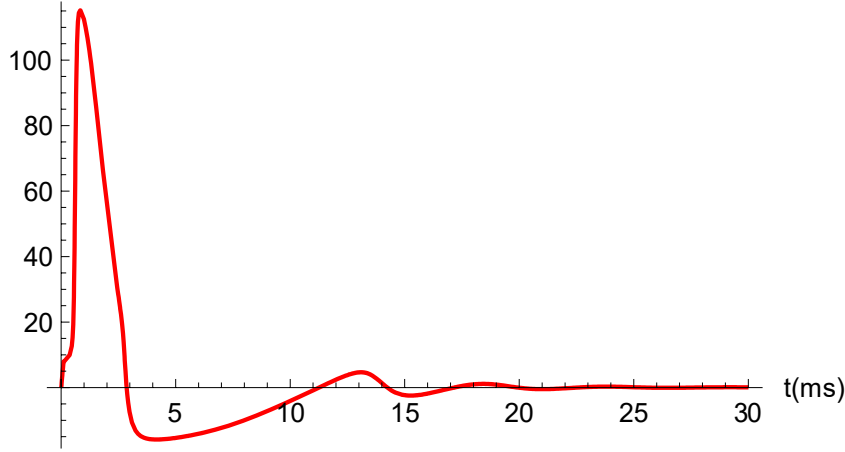
**B** action potential  $V(t)$  (mV)

Fig. 4. Membrane action potential at  $20^{\circ}\text{C}$  induced by a depolarizing current density pulse of constant strength  $-80 \mu\text{A m}^{-2}$  applied transversely for 0.1 ms at  $t = 0$  ms.

We discussed earlier (see Fig. 1B) the action potential predicted by our model in response to a brief hyperpolarizing current stimulus.

### 2.3 Propagating Action Potentials

Symbolic, numerical and graphical capabilities of Wolfram's Mathematica software permit the standard HH cable equation (13) in conjunction with our gating equations

$$\frac{\partial m(z,t)}{\partial t} = \frac{m_{\text{ss}}[V(z,t)] - m(z,t)}{\tau_m}, \quad (15a)$$

$$\frac{\partial h(z,t)}{\partial t} = \frac{h_{\text{ss}}[m(z,t)] - h(z,t)}{\tau_h}, \quad (15b)$$

and

$$\frac{\partial n(z,t)}{\partial t} = \frac{n_{\text{ss}}[V(z,t)] - n(z,t)}{\tau_n}, \quad (15c)$$

and (3)-(6) to be solved routinely by using the method of lines. Here, the steady state gating functions are the expected generalizations of (12) with  $V \equiv V(z,t)$ ,  $m \equiv m(z,t)$ ,  $h \equiv h(z,t)$  and  $n \equiv n(z,t)$ . The initial values of the gating functions are  $m(z,0) = m_{\text{ss}}[V(z,0)] = m_{\text{rest}}$ ,  $h(z,0) = h_{\text{ss}}[m(z,0)] = h_{\text{rest}}$  and  $n(z,0) = n_{\text{ss}}[V(z,0)] = n_{\text{rest}}$ , with  $V(z,0) = 0$ . To estimate propagation speeds, we have considered a 10 cm section of a squid giant axon with an internal axial resistivity [1] of  $R = 35.4$  ohm cm and an axially homogeneous radius [1] of 0.238 mm. The initial condition corresponds to the resting axon as described in Table 1 with all transmembrane pumps switched off. A propagating impulse can then, for example, be

initiated according to the boundary condition (14a) at  $z = 0$ , by a constant longitudinal current density pulse  $i_{z,\text{stim}}$  of  $7.8 \text{ A m}^{-2}$  applied for  $0.50 \text{ ms}$  at  $t = 0.01 \text{ ms}$ . The influence of such a stimulating current on the axonal membrane is clearly depolarizing for  $z > 0$  just after the stimulus ceases. The second boundary condition (14b) stipulates zero axial electric current density at  $z = 10 \text{ cm}$ . A graphical solution to these equations is presented in Fig. 5.

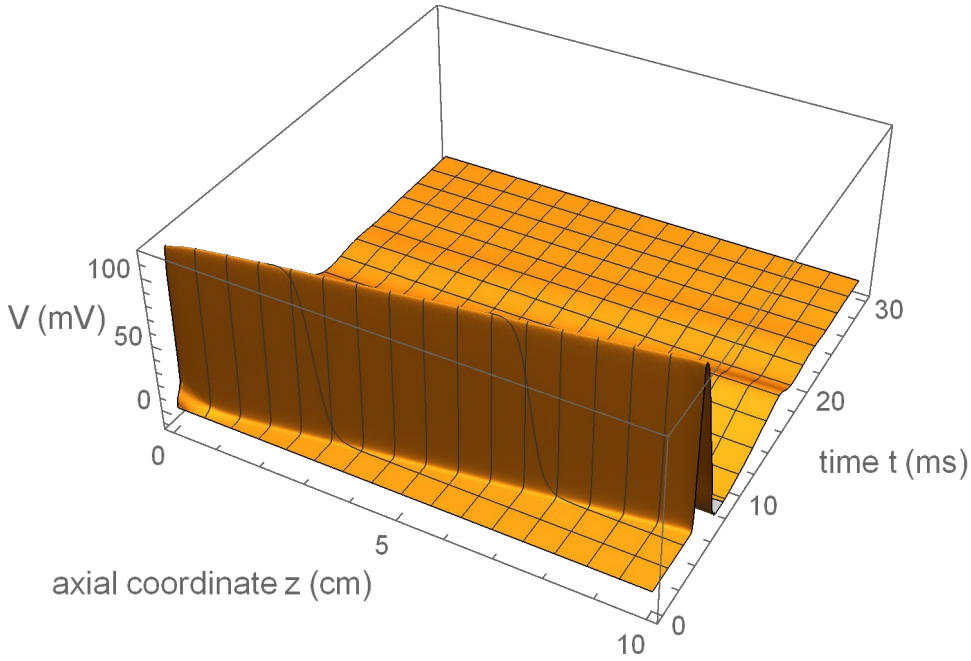


Fig. 5. Plot of an action potential  $V(z,t)$  of peak height  $118.7 \text{ mV}$  propagating at  $20^\circ\text{C}$  from left to right along a  $10 \text{ cm}$  section of squid axon, and induced between  $t = 0.01 \text{ ms}$  and  $t = 0.51 \text{ ms}$  by a rectangular pulse at  $z = 0$  of stimulating current density  $i_{\text{stim}} = 7.8 \text{ A m}^{-2}$ , also directed from left to right. From analysis of this result we find a propagation speed of  $21.1 \text{ ms}^{-1}$ , at  $20^\circ\text{C}$ , in excellent agreement with the estimated experimental speed [1] of  $21.2 \text{ ms}^{-1}$  at  $18.5^\circ\text{C}$ .

As pointed out by Jack *et al.* [35] the speed of a nerve impulse is faster close to the stimulated end of a finite axon with uniform diameter but, for a long axon, rapidly becomes spatially homogeneous as we move away from the boundaries. The propagation speed of  $21.1 \text{ ms}^{-1}$  indicated in Fig. 5 was estimated from the time taken for the peak of our action potential to travel from  $z = 4.95 \text{ cm}$  to  $z = 5.05 \text{ cm}$ .

If the initial and boundary conditions described above are applied to either the HH model or to the present electrodiffusion model, the direction and duration of our constant stimulating axial current required to elicit right-propagating action potentials become crucial issues. As shown in Fig. 5, initiation of a normal propagating action potential by a positive electric current density applied for  $0.5 \text{ ms}$  at  $z = 0$  usually requires a superthreshold axial current density with constant magnitude of at least  $7.8 \text{ A m}^{-2}$ . This positive electric current density, associated with cations moving from left to right or with anions moving from right to left, depolarizes the axonal membrane for all  $z > 0$ . When the magnitude of this stimulating current density  $i_{\text{stim}}(0,t)$  is sufficiently large, transient subthreshold oscillations resonate and

an action potential fires [9]. If, on the other hand, a much stronger negative longitudinal current-density pulse  $i_{\text{stim}}(0, t) = -69 \text{ A m}^{-2}$  is applied to the squid axon at  $z = 0$  between  $t = 0.01 \text{ ms}$  and  $t = 0.51 \text{ ms}$  the neural membrane of the squid axon first hyperpolarizes. Immediately after this hyperpolarizing pulse of stimulating current ceases the membrane at  $z > 0$  depolarizes rapidly, resonates, and fires as illustrated in Fig. 6 below. An inhibitory rebound propagating action potential, with a profile similar to that of the space-clamped action potential displayed in Fig. 1B, is produced and propagates along the positive  $z$  direction. As noted earlier, we are unaware of experimental investigations of propagating action potentials induced solely by such brief hyperpolarizing axial currents in giant axons of squid.

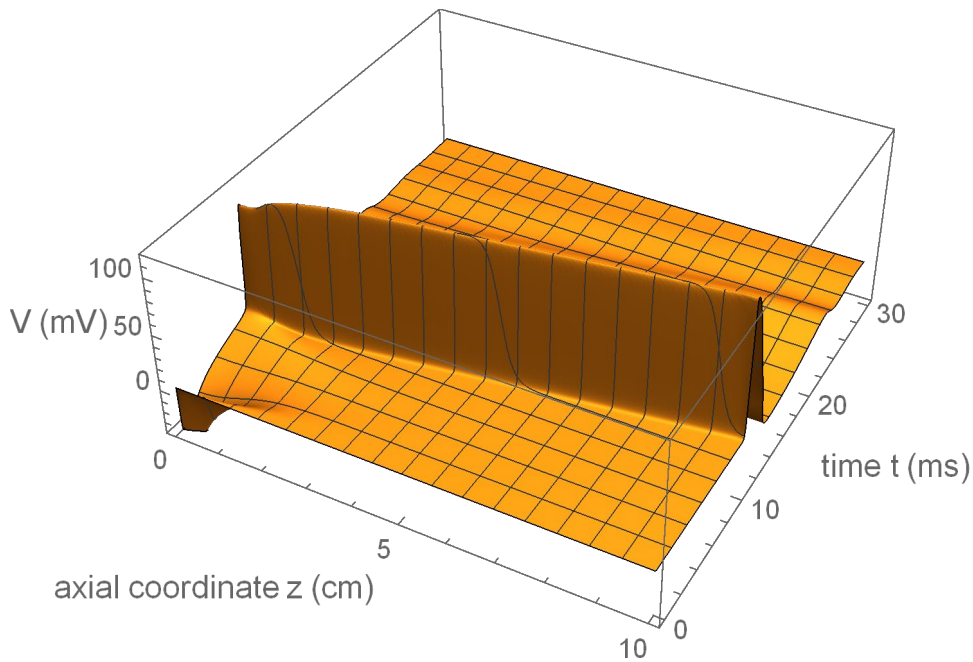


Fig. 6. An action potential with a significant latency is predicted by our electrodiffusion model when the left hand side boundary condition at  $z = 0$  is a constant  $-69 \text{ A m}^{-2}$  stimulating axial current density directed from right to left for 0.5 ms. The speed of the left-to-right propagating action potential, with a peak depolarization of 119 mV, is  $22.1 \text{ ms}^{-1}$  at  $20^\circ\text{C}$ .

### 3. Concluding Remarks

We have extended the quantitatively crude but simple and physically based nonlinear GHK model, for resting potentials in the giant axon of the squid, into the time domain. This has enabled us to describe both stationary space fixed and propagating action potentials more naturally by avoiding speculative gating-state dependencies, such as  $m^3h$  and  $n^4$ , introduced by HH to quantify ionic current densities in voltage-gated sodium and potassium channels. Our very simple theoretical model provides a unified nonlinear treatment of both resting and action potentials in perfused [14] giant axons of squid in which the intact axoplasm of a live squid has been replaced by its original contents minus the ATP required to

power various pumps. We have also confirmed that voltage-dependent relaxation times for channel-gating, used in the HH model, are dispensable [10]. This model can be extended to describe resting and action potentials for axons with pumps on. To model a live squid the external electrolyte should also have the composition of cephalopod blood in which the external potassium ion concentration is roughly double that of sea water [33].

The chloride ion concentration within the giant axon requires careful consideration. It was originally measured by Steinbach [42] who obtained the value 40 mM that was subsequently endorsed by Hodgkin [33]. This internal concentration is very similar to that expected if the chloride ions are passively distributed, in compliance with the Nernst equation, across the squid axolemma. Subsequent experimental investigations, however, by Koechlin [43] and by Keynes [44] yielded estimates of about 140 mM and 123 mM, respectively, that have been strongly supported by the subsequent discovery of the ATP-linked sodium-potassium-chloride cotransporter [45] which functions as an electrically silent chloride ion pump. If our perfused squid axon contains no ATP, so that both the Na-K-ATPase pumps and the chloride ion cotransporter pumps are switched off, the internal chloride ion concentration of 40 mM recommended by Hodgkin [33] seems most appropriate for our present calculations on electrodiffusion. We then predict a resting potential  $V_m$  of about  $-68$  mV, a membrane action potential with peak depolarization close to 119 mV at  $20^\circ\text{C}$  and speeds of propagating action potentials very close to those determined experimentally by HH on a squid axon that was not internally perfused.

Unlike its HH counterpart, our new theoretical model for perfused axons does not, in agreement with recent experiments [3], predict spike trains during prolonged constant-current stimulation. Our electrodiffusion model in resonator form predicts rebound spiking following prolonged hyperpolarizing stimulation, observed at  $18.5^\circ\text{C}$  by HH but not predicted at this temperature by their own quantitative model. Spiking promoted by brief (0.1 ms) hyperpolarization is also predicted at room temperature by our electrodiffusion model but only at much lower temperatures (*ca.*  $6^\circ\text{C}$ ) by the HH model. Such spiking induced directly by brief hyperpolarizing stimulation at room temperature does not yet appear to have been investigated experimentally in giant axons, either for stationary membrane action potentials or for their propagating counterparts.

Finally we mention that by simultaneously varying several of the parameters in the present resonator version of our electrodiffusion model from their values in Table 1, while demanding steeper steady-state gating functions in Fig. 2 and (12), we can switch the qualitative behavior of our electrodiffusion model from resonator firing, encountered in squid and diverse neurons of mammalian brains, to experimentally less ubiquitous integrator firing [6,7]. Far more elaborate molecular dynamics models, incorporating detailed kinetics of ATPase ion pumps, detailed structural features of ion channels, more realistic spatio-temporal electrolyte distributions within ion channels and extending beyond their orifices can be envisaged for an *in-vivo* axonal membrane. We suspect, however, that our present GHK-inspired nonlinear refinement of the basically electrodiffusive HH phenomenological model for a perfused squid axon captures the simple physics essential for understanding both resting and action potentials.

## References

- [1] Hodgkin, A.L. and Huxley, A.F. A quantitative description of membrane current and its application to conduction and excitation in nerve. *J. Physiol. (London)*, **117**, 500-544 (1952).
- [2] Hodgkin, A.L., Huxley, A.F. and Katz, B. Measurement of current-voltage relations in the membrane of the giant axon of *Loligo*. *J. Physiol.(London)*, **116**, 424-448 (1952).
- [3] Clay, J.R. Excitability of the squid giant axon revisited. *J. Neurophysiol.* **80**, 903-913 (1998).
- [4] Best, E.N., Null space in the Hodgkin-Huxley equations. A critical test. *Biophys. J.* **27**, 87-104 (1979).
- [5] Chapman, R.A. Repetitive responses in squid giant axons. *Quart. J. Exp. Physiol.* **65**, 1-7 (1980).
- [6] Integrator versions of our electrodiffusion model exhibit overdamped exponential relaxation after the axon, initially in its resting state, experiences an impulsive subthreshold electric perturbation. They eschew subthreshold oscillatory relaxation in the membrane potential which is characteristic of resonators.
- [7] Izhikevich, E.M. *Dynamical Systems in Neuroscience*, pp. 218-224, 248-249 (MIT Press, Cambridge MA, 2007).
- [8] Dodla, R., Svirskis, G. and Rinzel, J. Well-timed, brief inhibition can promote spiking: postinhibitory facilitation. *J. Neurophysiol.* **95**, 2664-2677 (2006).
- [9] Izhikevich, E.M. Resonate-and-fire neurons. *Neural Networks*, **14**, 883-894 (2001).
- [10] Perram, J.W. and Stiles, P.J. A dynamical system for action potentials in the giant axon of the squid. *J. Phys. Chem. C*, **114**, 20350-20361 (2010).
- [11] Goldman, D.E. Potential, impedance and rectification in membranes. *J. Gen. Physiol.* **27**, 37-60 (1943).
- [12] Hodgkin, A. L. and Katz, B. The effect of sodium ions on the electrical activity of the giant axon of the squid. *J. Physiol. (London)*, **108**, 37-77 (1949).
- [13] Perram, J.W. and Stiles, P.J. On the nature of liquid junction potentials and membrane potentials. *Phys. Chem. Chem. Phys.* **8**, 4200-4213 (2006).
- [14] Baker, P.F., Hodgkin, A.L. and Shaw, T.I. Replacement of the protoplasm of a giant nerve fibre with artificial solutions. *Nature* **190**, 885-887 (1961), and The effects of changes in internal concentrations on the electrical properties of perfused giant axons. *J. Physiol. (London)*, **164**, 355-374 (1962).
- [15] Läuger, P. *Electrogenic Ion Pumps*, Chapter 8 (Sinauer Associates, Sunderland, MA, 1991).
- [16] Morth, J.P., Pederson, B.P., Toulstrup-Jensen, M.S., Sorenson, T. L-M., Petersen, J., Andersen, J.P., Vilsen, B. and Nissen, P. Crystal structure of the sodium-potassium pump. *Nature* **450**, 1043-1049 (2007).
- [17] Gadsby, D.C., Takeuchi, A., Artigas, P. and Reyes, N. Peering into an ATPase ion pump with single channel recordings. *Philos. Trans. R. Soc. (London) B*, **364**, 229-238 (2009).
- [18] Mullins, L.J. and Noda, K. The influence of sodium-free solutions on the membrane potential of frog muscle fibers. *J. Gen. Physiol.* **47**, 117-132 (1963).
- [19] Frankenhaeuser, B. and Huxley, A.F. The action potential in the myelinated nerve fiber of *Xenopus Laevis* as computed on the basis of voltage clamp data. *J. Physiol. (London)*, **171**, 302-315 (1964).
- [20] See [10], that describes an integrator model with complicated PMFs. It finds an  $I-V$  curve with three fixed points rather than one, with just one being determined experimentally [2].

- [21] Hille, B. *Ion Channels of Excitable Membranes*, p. 454, 3<sup>rd</sup> ed., (Sinauer, Sunderland, MA, 2001).
- [22] Moore, J.W. and Cole, K.S. Resting and action potentials of the squid giant axon *in vivo*. *J. Gen. Physiol.* **43**, 961-970 (1960).
- [23] Fitzhugh, R. Mathematical models of threshold phenomena in the nerve membrane. *Bull. Math. Biophys.* **17**, 257-278 (1955).
- [24] Cole, K.S., Guttman, R. and Bezanilla, F. Nerve membrane excitation without threshold. *Proc. Nat. Acad. Sci.* **65**, 884-891 (1970).
- [25] Bezanilla, F. and Armstrong, C.M. Inactivation of the sodium channel. I Sodium current experiments. *J. Gen. Physiol.* **70**, 549-566 (1977).
- [26] Vandenberg, C.A. and Bezanilla, F. A sodium channel gating model based on single channel, macroscopic ionic and gating currents in the squid giant axon. *Biophys. J.* **60**, 1511-1533 (1991).
- [27] Patlak, J. Molecular kinetics of voltage-dependent  $\text{Na}^+$  channels. *Physiol. Rev.* **71**, 1047-1080 (1991).
- [28] Delemotte, L., Kasimova, M.A., Klein, M.L., Tarek, M. and Carnevale, V. Free-energy landscape of ion-channel voltage-sensor-domain activation. *Proc. Nat. Acad. Sci.* **112**, 124-129, (2015).
- [29] Linaeus, M.J., El-Din, T.M.G., Ing, C., Ramanadane, K. Pomès, R., Zheng, N. and Catterall, W.A. Structures of closed and open states of a voltage-gated sodium channel. *Proc. Nat. Acad. Sci.* **114**, E3051-E3060, (2017).
- [30] Aidley, D.J. *The Physiology of Excitable Cells*. 4<sup>th</sup> ed. Chapter 6, (Cambridge University Press, Cambridge, 1998).
- [31] Payandeh, J., Scheuer, T., Zheng, N. and Catterall, W.A. The crystal structure of a voltage-gated sodium channel. *Nature*, **475**, 353-358 (2011).
- [32] Jiang, Y., Lee, A., Chen, J., Ruta, V., Cadene, M., Chait, B.T. and MacKinnon, R. X-ray structure of a voltage-dependent  $\text{K}^+$  channel. *Nature* **423**, 33-41 (2003).
- [33] Hodgkin, A.L. Ionic movements and electrical activity in giant nerve fibres. *Proc. R. Soc. (London) B* **148**, 1-37 (1958).
- [34] Bezanilla, F. Gating currents. *J. Gen. Physiol.* **150**, 911-932 (2018).
- [35] Jack, J.J.B., Noble, D. and Tsien, R.W. *Electric Current Flow in Excitable Cells* (Clarendon Press, Oxford, 1975).
- [36] Inoue, I. Voltage-dependent chloride conductance of the squid axon membrane and its blockade by some disulfonic stilbene derivatives. *J. Gen. Physiol.* **85**, 519-537 (1985).
- [37] Jackson, M.B. *Molecular and Cellular Biophysics*, p.390, (Cambridge University Press, Cambridge, 2006).
- [38] Nelson, P.H. A permeation theory for single-file ion channels: one-and two-step models. *J. Chem. Phys.* **134**, 165102-1-13 (2011).
- [39] Hodgkin, A.L. and Keynes, R.D. The potassium permeability of a giant nerve fibre. *J. Physiol.* **128**, 61-88 (1955).
- [40] Tolokh, I.S., Goldman, S. and Gray, C.G. Unified modeling of conductance kinetics for low- and high-conductance potassium ion channels. *Phys. Rev. E* **74**, 011902-1-12 (2006).
- [41] Köpfer, D.A., Song, C., Gruene, T., Sheldrick, G.M., Zachariae, U. and de Groot, B.L. Ion permeation in  $\text{K}^+$  channels occurs by direct Coulomb knock-on. *Science* **346**, 352-355 (2014).
- [42] Steinbach, H.B. Chloride in the giant axons of squid. *J. Cell. Comp. Physiol.* **17**, 57-64 (1941).

- [43] Koechlin, B.A. On the chemical composition of the axoplasm of squid giant nerve fibers with particular reference to its ionic pattern. *J. Biophys. Biochem. Cytol.* **1**, 511-529 (1955).
- [44] Keynes, R.D. Chloride in the squid giant axon. *J. Physiol.* **169**, 690-705 (1963).
- [45] Russell, J.M. Sodium-potassium-chloride cotransport. *Physiol. Rev.* **80**, 211-276 (2000).